Check for updates

Calcification and trophic responses of mesophotic reefs to carbonate chemistry variability

Timothy J. Noyes[1,2]*, Rebecca Garley[2]
and Nicholas R. Bates[2]

[1]School of Science, Engineering and Environment, University of Salford, Manchester, United Kingdom,
[2]Bermuda Institute of Ocean Sciences, Arizona State University, St. George's, Bermuda

Mesophotic coral ecosystems (MCEs) are extensions of adjacent shallow water coral reefs. Accessibility to these ecosystems is challenging due to their depth limits (~ 30 − 150 m) and as a result, scientific knowledge of these reef systems is limited. It has been posited that the depth limits of MCEs diminish anthropogenic effects experienced by shallow reef systems. A lack of empirical measurements to date has made this hypothesis impossible to determine for mesophotic reef metabolism. The alkalinity anomaly technique was utilized to determine rates of net ecosystem calcification (NEC) and net ecosystem production (NEP) from 30, 40 and 60 m mesophotic reefs during a 15-month period. Seawater chemistry was determined to be chemically conducive for calcification (average aragonite saturation $\Omega_{aragonite}$ of 3.58, average calcite saturation $\Omega_{calcite}$ of 5.44) with estimates of NEC indicating these reef systems were net accretive and within global average values for shallow coral reefs (< 30 m). The strongest periods of calcification occurred in late summer and were coupled with strong autotrophic signals. These episodes were followed by suppressed calcification and autotrophy and in the case of the 60 m reefs, a switch to heterotrophy. Whilst there was variability between the three reefs depths, the overall status of the mesophotic system was net autotrophic. This determination was the opposite of trophic status estimates previously described for adjacent shallow reefs. Whilst there were periods of net dissolution, the mesophotic reef system was net accretive (i.e., gross calcification > gross $CaCO_3$ dissolution). The measured inorganic carbon chemistry and estimates of NEC and NEP represent the first such biogeochemical measurements for MCEs. The values established by this study demonstrate just how close these understudied ecosystems are in terms of the known boundary thresholds for low saturation state reefs. Making predictions on how these ecosystems will respond to future climatic conditions, will require greater sampling effort over long times scales to decouple the environmental controls exerted on such ecosystems.

1 Introduction

Coral reefs are highly diverse marine ecosystems forming complex three-dimensional frameworks, generated through biogenically precipitated calcium carbonate ($CaCO_3$) primarily produced by hermatypic corals, calcareous algae and foraminifera. Such calcification is responsible for ~50% of net annual $CaCO_3$ oceanic precipitation (Dubinsky and Stambler, 2011). Globally, coral reef ecosystems provide numerous socio-economic and ecological functions (Moberg and Folke, 1999; Sarkis et al., 2013). Their global decline through disturbance events, climate change and a myriad of anthropogenic activities have been well documented in the literature (e.g., (Wilkinson, 1999; Jackson et al., 2001; Pandolfi et al., 2003; Hughes et al., 2007; Wilkinson, 2008; Hoegh-Guldberg, 2011; Tanzil et al., 2013; Jackson et al., 2014). These declines have led to increased scientific interest in deeper reef ecosystems (e.g., mesophotic, generally deeper than 30 m) that may exhibit reduced susceptibilities and greater resistance to such environmental change (Glynn, 1996; Puglise et al., 2008; Bongaerts et al., 2010; Baker et al., 2016; Cinner et al., 2016; Loya et al., 2016; Bongaerts et al., 2017; Semmler et al., 2017; Turner et al., 2017).

Deeper reef systems (generally deeper than 30 m with depths up to ~ 150 m) termed "mesophotic coral ecosystems" (MCEs; Hinderstein et al., 2010) have a near-ubiquitous presence below shallow coral reefs (Bridge et al., 2013). The consensus within the research community is that MCEs are often extensions of shallow coral reef systems (Hinderstein et al., 2010; Pyle et al., 2019 and references therein) with common species shared between the two communities. Subdivisions of the MCE habitat based on biodiversity changes across depth have been proposed (Pyle et al., 2019 references therein). It is this commonality of species combined with the suggestion that MCEs could be buffered from anthropogenic influence (e.g., ocean warming and acidification) and natural disturbances (Bongaerts et al., 2013; Loya et al., 2016) that makes these ecosystems of particular scientific interest. Determining the levels of oceanographic connectivity between mesophotic and adjacent shallow-water reefs has become a key research priority across disciplines (e.g., biogeochemistry, marine spatial planning). Given that biological carbonates are the largest carbon reservoirs in the biosphere (i.e., aragonite, calcite, and magnesian calcite; Cohen, 2003), to truly comprehend the level of resilience coral reef systems have too anthropogenic and natural stressors, understanding the interactions and feedbacks that drive these biogeochemical processes (e.g., calcification rates, thermal regimes, flow dynamics) are fundamental requirements. Oceanic uptake of anthropogenic CO_2 has led to significant changes in seawater chemistry (Orr et al., 2005) which in turn has raised concerns about the consequences to marine calcifiers (e.g., hermatypic corals, calcareous algae and foraminifera; Kleypas et al., 1999; Hoegh-Guldberg et al., 2007) to generate and maintain $CaCO_3$ structures through a reduction in seawater pH and aragonite saturation state ($\Omega_{aragonite}$; Cyronak et al., 2018; Eyre et al., 2018). Of equal importance is the potential for rates of bioerosion and dissolution of $CaCO_3$ structures (Andersson et al., 2009; Tribollet et al., 2009; Dove et al., 2013) to increase under the same conditions. The persistence of coral reefs is dependent on their ability to calcify and produce $CaCO_3$ and maintain net positive accretion (Equation 1). At reef scale, net accretion of $CaCO_3$ and external sediment supply (e.g., broken down framework, shells) must be greater than any loss by dissolution, transport, or erosion (Kleypas et al., 2001; Andersson and Gledhill, 2013; Eyre et al., 2018).

$$CaCO_3 \text{ accretion}$$
$$= CaCO_3 \text{ production} - CaCO_3 \text{ dissolution}$$
$$- \text{ physical loss of } CaCO_3 \quad (1)$$

Both models and mesocosm studies on individual and community calcifiers have measured decreased rates in calcification (net accretion) and increases in $CaCO_3$ dissolution ultimately transitioning to a state of net dissolution under projected atmospheric and seawater CO_2 conditions (Pandolfi et al., 2011; Andersson and Gledhill, 2013; Lantz et al., 2014). However, there is considerable uncertainty as to when this inferred threshold may be crossed (Andersson and Gledhill, 2013). Rates of net coral $CaCO_3$ production can be determined through chemistry-based methods (i.e., net ecosystem calcification [NEC] = gross calcification – gross $CaCO_3$ dissolution) and can provide a top-down integrated measurement of the entire reef NEC (Courtney et al., 2016). Modification of CO_2-carbonate chemistry of Bermudan mesophotic reefs will reflect the main biogeochemical processes occurring on the reef system (Bates, 2002; Bates et al., 2010; Andersson et al., 2014; Yeakel et al., 2015; Courtney et al., 2016; Bates, 2017). It is accepted that inorganic $CaCO_3$ accretion occurs at seawater saturation state (Ω) >1 whereas the dissolution of $CaCO_3$ occurs when Ω<1. However, biogenic reef carbonate dissolution has been determined to occur well above this expected thermodynamic transition value (Langdon et al., 2000; Bates et al., 2010; Andersson et al., 2014).

In this study, we characterized mesophotic reef CO_2-carbonate chemistry between August 2017 and October 2018 across a depth gradient (30 m, 40 m, and 60 m) at three locations in Bermuda (Figure 1). In situ mesophotic seawater carbonate chemistry measurements were compared to contemporaneous measurements taken from the long-term Bermuda Atlantic Time-series Study (BATS). In addition to carbonate chemistry measurements, in situ temperature, salinity and inorganic nutrients were characterized at the study sites. Mesophotic NEC was derived using the alkalinity anomaly-water residence time technique (Langdon et al., 2010) to investigate spatial and temporal variability in calcification and compared to historic Bermuda NEC shallow reef measurements. Rates of NEP were calculated to determine the trophic status of the Bermuda mesophotic reef system (i.e., net heterotrophy or net autotrophy). The characterization of CO_2-carbonate chemistry and estimates of NEC and NEP provide valuable insight to the biogeochemical status of these understudied ecosystems.
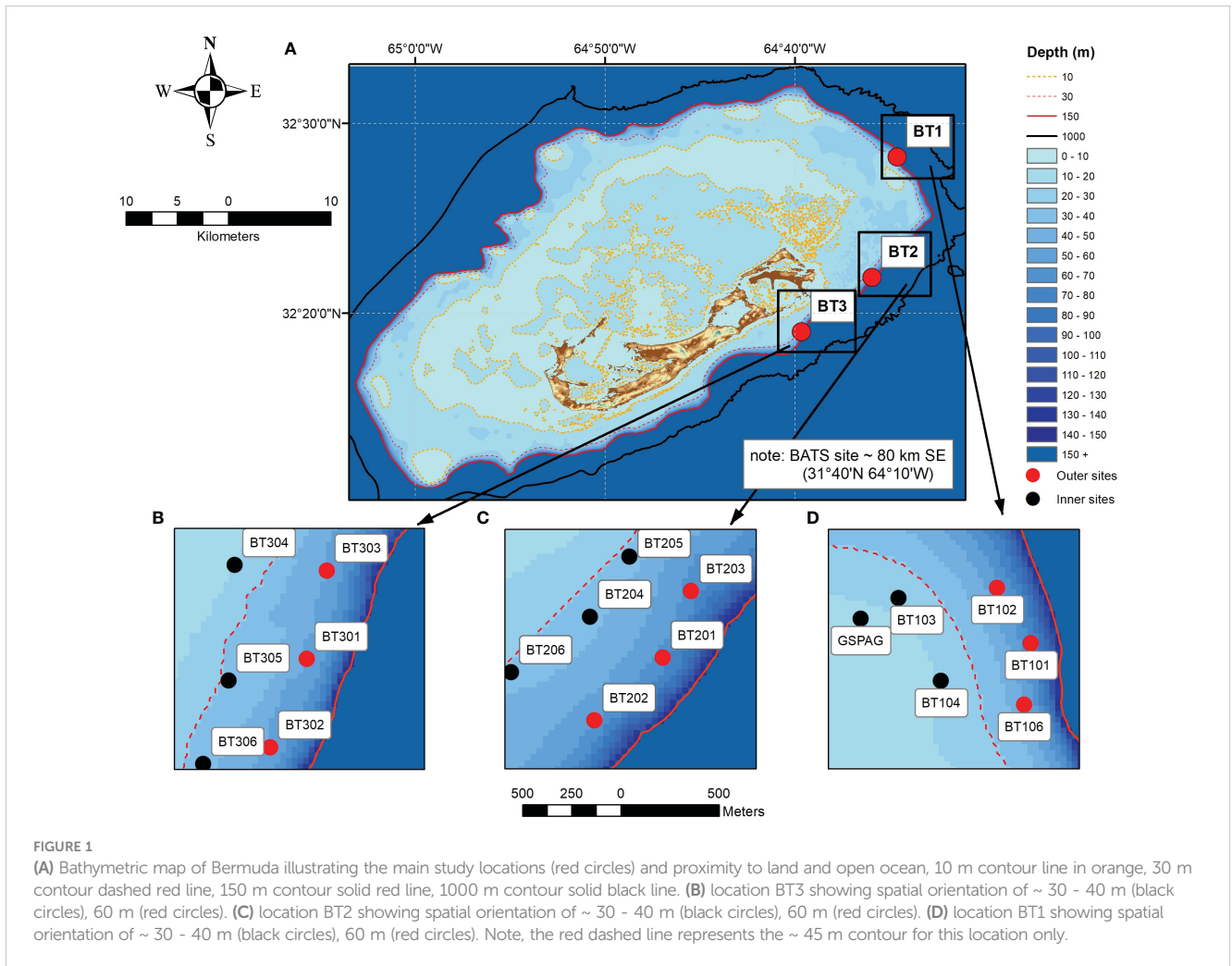
FIGURE 1
(A) Bathymetric map of Bermuda illustrating the main study locations (red circles) and proximity to land and open ocean, 10 m contour line in orange, 30 m contour dashed red line, 150 m contour solid red line, 1000 m contour solid black line. **(B)** location BT3 showing spatial orientation of ~ 30 - 40 m (black circles), 60 m (red circles). **(C)** location BT2 showing spatial orientation of ~ 30 - 40 m (black circles), 60 m (red circles). **(D)** location BT1 showing spatial orientation of ~ 30 - 40 m (black circles), 60 m (red circles). Note, the red dashed line represents the ~ 45 m contour for this location only.

2 Methodology

2.1 Study locations

Bermuda is located approximately 1000 km east south-east of the United States of America (Jones et al., 2012) in the northwest of the Sargasso Sea (Coates et al., 2013) and considered the northernmost reefs of the Atlantic (Spalding et al., 2002; Logan and Murdoch, 2011). Bermuda's coral reef system transitions through a series of shallow patch reefs, shallow rim reefs, and terraced reefs (Logan, 1988; Logan and Murdoch, 2011) dropping quickly to deeper mesophotic reefs that surround the main reef platform (Goodbody-Gringley et al., 2019). Using the 30 – 150m contours in a Bermuda 1 arc-second sea level digital elevation model (Sutherland et al., 2014) as a proxy for the extent of the mesophotic zone surrounding Bermuda, the system covers 76 km^2 which equates to 8% of habitats< 30 m (908 km^2). All physiographic reef zones are influenced by the offshore waters from the Sargasso Sea (Steinberg et al., 2001; Bates, 2017). The study was performed on three mesophotic reef locations between August 2017 and October 2018 (Figure 1). The choice of locations were defined a posteriori following the findings of a Darwin Plus (DPLUS001) lionfish control initiative project completed in 2015. At each location, a grid of six sites approximately ~ 350 m apart were arranged in a pattern of three shallow (30 ~ 40 m) and three deep sites (60 m). The benthic community composition followed the pattern reported by Fricke and Meischner (1985) and was expanded upon in the review of Bermuda's mesophotic reefs by Goodbody-Gringley et al. (2019). Moving in a seaward direction, shallow mesophotic sites (~30 m depth) were dominated by hermatypic scleractinian corals whilst the deeper sites exhibited greater benthic heterogeneity as macroalgae (Stefanoudis et al., 2019) and rhodolith beds became more dominant.

2.2 Seawater carbonate chemistry determination

Carbon chemistry samples were collected on an ad hoc basis between August 2017 and October 2018 using a 12-liter water sampler bottle (Standard Model 110B, OceanTest Equipment, Inc.) at ~2 m above the benthos (Bates et al., 1996; Dickson et al., 2007). Comparative offshore samples were collected monthly as part of the Bermuda Atlantic Time-series Study (BATS; Bates et al., 2012). Samples for dissolved inorganic carbon (DIC; Equation 2) and total alkalinity (TA; Equation 3) were drawn into clean 300-ml Kimax glass sample bottles

and fixed with 100 µl of saturated mercuric chloride ($HgCl_2$) solution to prevent biological alteration. DIC was analyzed using an Automated InfraRed Inorganic Carbon Analyzer (AIRICA, Marianda Inc) or by coulometric technique on a VINDTA 3C system (Versatile INstrument for the Determination of Total Alkalinity, Marianda Inc; Courtney et al., 2016; Courtney et al., 2017). DIC is defined as Dickson et al. (2007) where $[CO_2^*]$ represents the concentration of all CO_2 whether as unionized as H_2CO_3 or CO_2:

$$DIC = [CO_2^*] + [HCO_3^-] + [CO_3^{2-}] \qquad (2)$$

All reef TA samples were analyzed via open-cell potentiometric titration with HCl of approximate normality of ~0.1 and ionic strength of ~0.7 using the VINDTA 3S system (Marianda Inc). The offshore BATS TA samples were analyzed on a VINDTA 2S system (Marianda Inc) with similar solutions. The VINDTA 2S system is the previous model of VINDTA 3S system and although it performs the same analytical function, BATS samples are preferentially run on this machine to maintain continuity, but with no demonstrable difference between analytical systems. TA is typically defined as:

$$TA = [HCO_3^-] + 2[CO_3^{2-}] + [B(OH)_4^-] + [OH-] + [HPO_4^{2-}] + 2[PO_4^{3-}] + [SiO(OH)_3^-] + [HS]+$$
$$[NH_3] + \quad minor \quad constituents - [H+] + [HSO_4^-] + [HF^-] - H_3PO_4] - minor \quad constituents$$
$$(3)$$

Seawater certified reference materials (CRMs; prepared by A.G. Dickson, Scripps Institution of Oceanography; http://www.dickson.ucsd.edu) were used to ensure the precision and accuracy of both DIC and TA values (typically ±1 to 2 µmoles kg^{-1}). For both reef and BATS measurements, seawater pH, pCO_2 and Ω were calculated using CO2SYS (Lewis and Wallace, 1998) from measured DIC and TA at in situ salinity and temperature conditions using the K1 and K2 dissociation constants from Mehrbach et al. (1973) refitted by Dickson and Millero (1987).

2.3 Physical and biogeochemical parameters

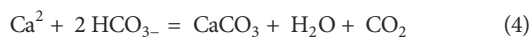Salinity samples were paired with all reef and BATS DIC and TA samples and collected in accordance with best practices (Knap et al., 1997). Samples were drawn into 250 ml clear borosilicate glass bottles with plastic screw caps. A plastic insert was used to form an airtight seal and stop sample evaporation. All samples were analyzed on a Guildline AutoSal 8400A laboratory salinometer (± 0.002) following the manufacturers recommendations for standard practices. Salinity measurements were calibrated against IAPSO standard seawater (Ocean Scientific, UK) to give a precision of ± 0.001-0.002 Practical Salinity Units (PSU). In situ temperatures were measured with an ONSET HOBO Water Temp Pro v2 (accuracy ±0.2°C between -40°C and 70°C). Inorganic nutrient samples were collected on an ad hoc basis (Table 1) at the central shallow and deep sites per each location only (Figure 1). Samples were collected following best practices (Knap et al., 1997), filtered through a 0.8 µm NucleporeTM filter (Whatman®) into prewashed 60 ml amber bottles (Nalgene® HDPE) stored on ice and immediately frozen on return to BIOS, prior to shipping to the Woods Hole Oceanographic Institution Nutrient Analytical Facility. All samples were analyzed on a SEAL Analytical AA3 HR Auto Analyzer using U.S. Environmental Protection Agency methods for ammonium (method G-171-96, detection limit 0.015 µmoles L^{-1}), nitrate + nitrate (method G-172-96, detection limit 0.040 µmoles L^{-1}), silicate (method G-177-96, detection limit 0.030 µmoles L^{-1}), and phosphate (G-297-03, detection limit 0.009 µmoles L^{-1}).

2.4 Determination of net ecosystem calcification and net ecosystem production

The determination of net ecosystem calcification (NEC; Equation 5; Gattuso et al., 1996) is based on the widely accepted alkalinity anomaly-water residence time technique (Smith and Key, 1975; Kinsey, 1978; Bates et al., 2010; Langdon et al., 2010; Andersson and Gledhill, 2013; Courtney et al., 2016; Bates, 2017; Courtney et al., 2017). The relative changes in DIC and TA reflect biogeochemical partitioning of carbon between the inorganic and organic cycles (Suzuki and Kawahata, 2003). The changes in DIC and TA as a result of NEC change in a ratio 1:2 DIC : TA. Net calcification (NEC > 0) will reduce both DIC and TA which causes a lowering of pH and $\Omega_{aragonite}$.

TABLE 1 Summary of the number of physico-chemical parameters measured at three reef zones.

Reef zone	Temperature	Salinity	DIC	TA	NH_4^+	$NO_2^- + NO_3^-$
30 m	38	38	38	38	17	17
40 m	41	41	41	41	17	17
60 m	98	98	98	98	33	33
Total	177	177	177	177	67	67
Reef zone	**PO_4^{3-}**	**Silicate**				
30 m	17	17				
40 m	17	17				
60 m	33	33				
Total	67	67				

$$Ca^2 + 2\,HCO_{3-} = CaCO_3 + H_2O + CO_2 \qquad (4)$$

Offshore BATS samples are assumed to be representative of waters flowing onto Bermudan mesophotic reefs. The sampling regimes between the MCE sites and BATS were typically conducted within 1-2 weeks of each other (Bates, 2017). To minimize the influence of isopycnal lifting as water transitions onto Bermuda MCEs, comparative offshore data were selected based on salinity and temperature. To account for local evaporation and precipitation changes, all (i.e., MCE and BATS) TA and DIC were salinity normalized, nTA and nDIC respectively, to a mean measured salinity of MCE reefs of 36.67 (Courtney et al., 2021).

The method assumes any differences in total alkalinity (TA) between offshore and mesophotic reef seawater (i.e., $nTA_{offshore} - nTA_{MCE}$) are a relative expression of MCE calcification and calculated as per the method of Langdon et al. (2010):

$$NEC = -0.5(nTA_{offshore} - nTA_{MCE}) \cdot (\sigma Z)/t \qquad (5)$$

Where σ is the density of seawater, Z is the depth of water and t is the water residence time for the mesophotic reef. Water depths for MCE sites were measured using a vessel mounted depth sounder (Garmin GPSmap 441s/Aimar P79 50/200 kHz transducer). Sample depths for offshore (BATS) samples were recorded by a Sea-Bird SBE 911 CTD instrument package (SBE 9 underwater unit, SBE 11 Deck unit). Sites were categorized as 30 m, 40 m and 60 m as determined by average depth measurements recorded over the duration of the study. Seawater residence times for mesophotic sites were deemed to be 0.5 days based on hydrological modelling (R. Johnson unpublished data). All discrete reef level samples were collected from ~ 2 m above the benthos, as such, any calcification and or dissolution signals (i.e., $CaCO_3$ precipitation/dissolution) are estimated to be detected within a 5 m^3 volume above the benthos. Rates of NEC are calculated in units of mmoles $CaCO_3$ m^{-2} d^{-1} (or expressed as g $CaCO_3$ m^{-2} d^{-1} using the molecular weight 100.09).

Net calcification (NEC > 0) draws down both DIC and TA causing a reduction in seawater pH and $\Omega_{aragonite}$ with resultant changes in DIC expressed as $\Delta nDIC^{NEC}$ (i.e., $\Delta nDIC^{NEC} = \Delta nTA^{NEC}/2$). NEP (Equation 6) alters DIC content of the water however, neither photosynthesis or respiration alter TA, therefore NEP is calculated as the difference between offshore BATS and onshore MCE samples as following the method of Bates (2017):

$$NEP = nDIC_{offshore} - nDIC_{MCE} - \Delta nDIC^{NEC} \qquad (6)$$

Air–sea CO_2 gas exchange were deemed minor relative to the calculations of NEC and NEP (Bates, 2017). Rates of NEP are calculated in units of mmoles C m^{-2} d^{-1} (or expressed as g C m^{-2} d^{-1} using a molecular weight of 12).

2.5 Propagation of uncertainty

Uncertainty for bottle NEC and NEP calculations were estimated using procedures outlined by Ku (1966). The uncertainty of measured DIC and TA (± 1 µmoles kg^{-1}) was obtained from routine measurement of CRMs (prepared by A.G.

Dickson, Scripps Institution of Oceanography; http://www.dickson.ucsd.edu) with the DIC and TA samples.

3 Results

3.1 Physical and biogeochemical variability

In total 177 paired comparisons were made between mesophotic reefs and reference samples taken at the BATS site which when delineated to depth categories, equated to 30 m = 38, 40 m = 41, 60 m = 98 samples respectively (Table 1). Monthly benthic seawater temperatures exhibited seasonal variability across all study sites ranging from 19.6 – 27.5 ± 2.2°C between winter and summer (Figures 2A–C). The summer monthly climatology of 60 m reefs tended to be ~ 3.5 to 4°C and ~ 2.5 to 3°C cooler than the 30 m and 40 m reefs respectively. Short term deployments (16 days, 15-minute intervals) of temperature loggers at 60 m sites recorded ~2 - 4°C daily variability (Figure 3). High degrees of thermal oscillation at mesophotic depths are known to occur (Wolanski et al., 2004; Colin, 2009; Colin and Lindfield, 2019) and have been attributed to internal waves. In the Pacific region of Micronesia, extreme daily thermal isolations at a 90 m depth (~ 20°C) were linked to a possible coupling of internal waves with a Rossby wave causing a deepening of the thermocline (Colin and Lindfield, 2019). Salinity across all mesophotic sites had a similar seasonal range to offshore values recorded at BATS 36.67 ± 0.09 g kg^{-1} (Figures 2D–F), however, samples from 2017 were slightly fresher than 2018 but still within the limits reported for the Bermuda environment (36.3 – 36.7; Coates et al., 2013; Yeakel et al., 2015). Inorganic nutrients concentrations were typically below 0.1 µmoles L^{-1} (oligotrophic water column; Table 2) and consistent with values previously published for Bermuda mesophotic reefs (Goodbody-Gringley et al., 2015). Approximately 50% of all inorganic nutrient measurements were below detection limits suggesting rapid uptake of dissolved inorganic nutrients and/or limited nutrient availability. Nutrient measurements were collected at a subset of sites (n = 67) over the duration of the study with a focus on the central 60 m site per location.

3.2 Temporal changes in seawater carbonate chemistry and trophic status

The 2017 monthly observations of nDIC (Figures 2G–I) at the shallow mesophotic sites (30 m, 40 m) were generally higher than values calculated from BATS (~3– 4 µmoles kg^{-1}). However, in 2018, the shallow reef observation fluctuated ± ~ 1 µmoles kg^{-1} around those observed at BATS. Observations from the 2017 60 m reefs fluctuated ± ~ 8 µmoles kg^{-1} around the BATS value whilst they were ~ 8 µmoles kg^{-1} higher than values observed at BATS in 2018. The mean nDIC values (± standard deviation) for BATS, the 30 m, 40 m and 60 m MCEs during this study period were 2069 ± 11 µmoles kg^{-1}, 2065 ± 10 µmoles kg^{-1}, 2067 ± 11 µmoles kg^{-1} and 2071 ± 14 µmoles kg^{-1} respectively. Generally, the mesophotic reefs had
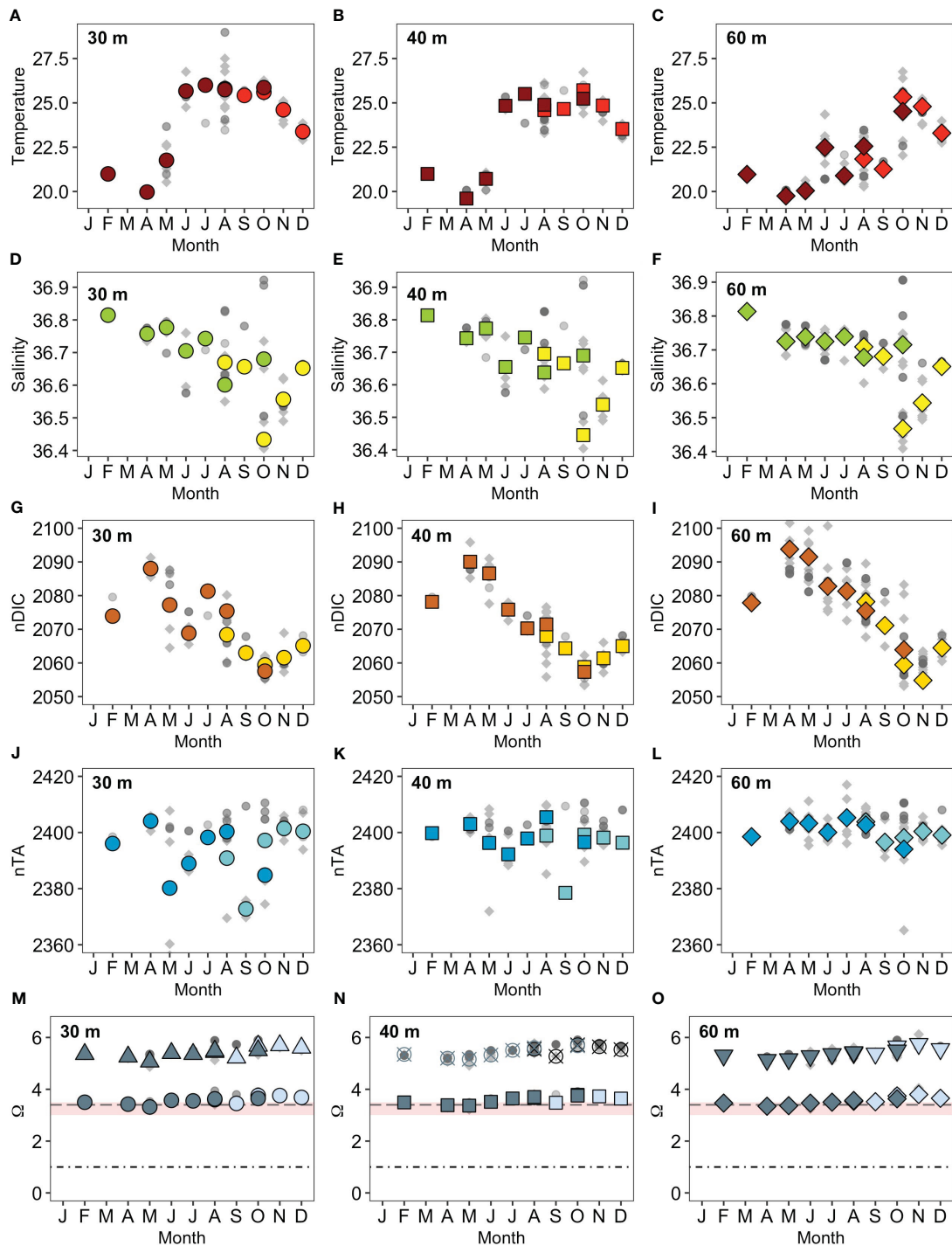
FIGURE 2

Mesophotic carbonate chemistry data at 30 m, 40 m and 60 m depths. **(A–O)**, BATS data (dark grey circles), MCE 2017 data (light grey circles), 2018 (grey diamonds). **(A–C)** Temperature °C (2017 red symbols, 2018 dark red symbols); **(D–F)** salinity PSU (2017 yellow symbols, 2018 green symbols); **(G–I)** nDIC (µmoles kg^{-1}, 2017 orange symbols, 2018 dark orange symbols); **(J–L)** nTA (µmoles kg^{-1}, 2017 blue symbols, 2018 dark blue symbols; **(M)** $\Omega_{aragonite}$ (2017 light blue circles, 2018 grey circles), $\Omega_{calcite}$ (2017 light blue triangles, 2018 grey triangles); **(N)** $\Omega_{aragonite}$ (2017 light blue squares, 2018 grey squares), $\Omega_{calcite}$ (2017 black hatched circles, 2018 light grey hatched circles); **(O)** $\Omega_{aragonite}$ (2017 light blue diamonds, 2018 grey diamonds), $\Omega_{calcite}$ (2017 light blue inverted triangles, 2018 grey inverted triangles). DIC, TA, $\Omega_{aragonite}$ and $\Omega_{calcite}$ have been salinity normalized to values of 36.67 g kg^{-1}. The black dot - dash line depicts $\Omega_{aragonite}$ = 1, thermodynamically, dissolution is anticipated if Ω< 1; grey dashed line depicts $\Omega_{aragonite}$ = 3.4, transition from coral reef to non-reef coral community; pink shaded area $\Omega_{aragonite}$ 3.0 − 3.5 defined as the global limit for reef development.
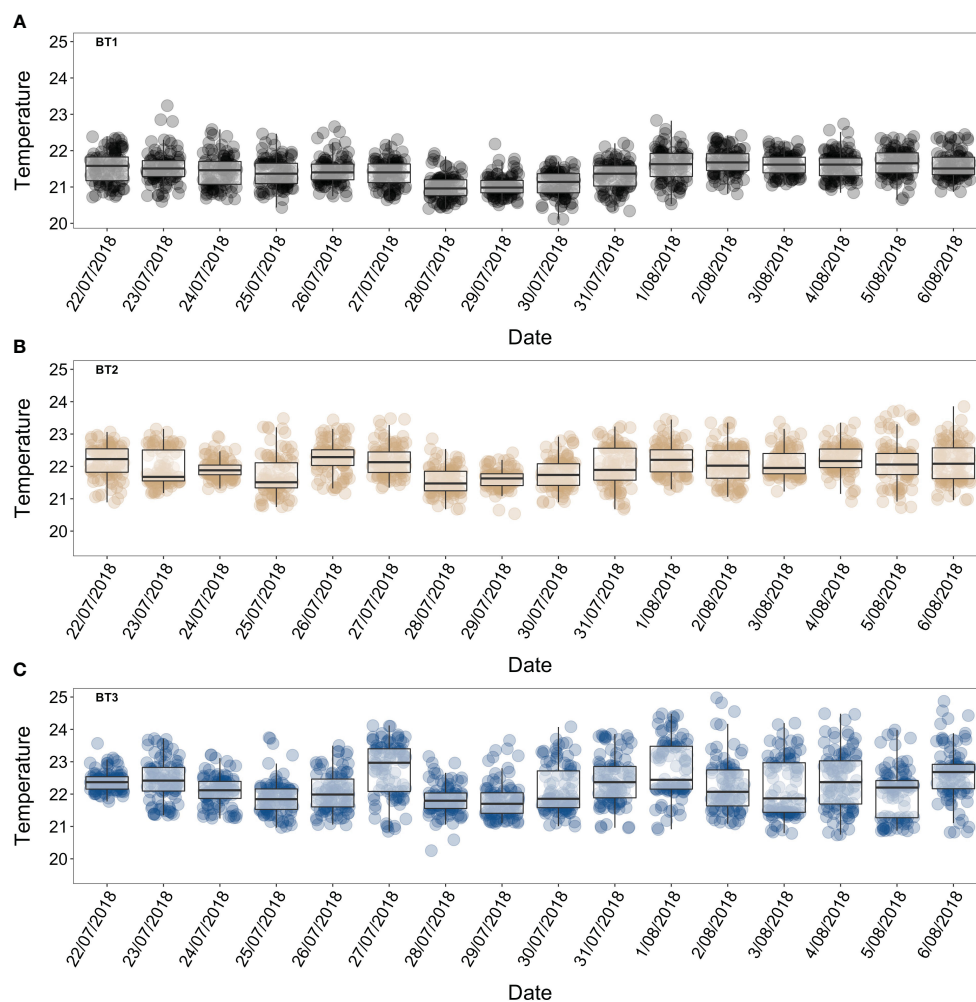
FIGURE 3
Boxplot of mean daily temperature °C (22nd July – 6th August 2018) at 60 m depths, boxes indicating 25th, 50th and 75th percentiles and whiskers show 5th and 95th percentiles. **(A)** BT1 (dark grey symbols), **(B)** BT2 (peril symbols), **(C)** BT3 (blue symbols).

lower nTA values than BATS for the duration of the study, with concentrations ranging between ~ 2 – 45 µmoles kg^{-1} lower. The mean nTA values (Figures 2J–L) for BATS, the 30 m, 40 m, 60 m and MCEs over this study period were 2399 ± 11 µmoles kg^{-1}, 2389 ± 13 µmoles kg^{-1}, 2394 ± 8 µmoles kg^{-1} and 2397 ± 5 µmoles kg^{-1} respectively. The values recorded from mesophotic reefs followed the seasonal pattern recorded at BATS for both nDIC and nTA (Figures 2G–L). The saturation states for aragonite ($\Omega_{aragonite}$) and calcite ($\Omega_{calcite}$) remained stable for the duration of the study (Figures 2M–O).

With the exception of the 60 m reefs, the monthly mean NEP of MCEs exhibited similar albeit, inverted (i.e., decreases of NEP coincided with increases in NEC; Figure 4) seasonal patterns to those observed for NEC. There were seasonal differences in NEP signals recorded from the three reef zones (H = 17.144, p =<0.0001; Table 3) that reflected the trophic switch over the course of the year (Figures 4B, D, F). NEP did not differ across the three reef zones (H = 3.728, p = 0.155) despite the observed differences in the monthly mean patterns. Between May and December, the 30 – 40 m NEP values were generally negative and symptomatic of autotrophy (photosynthesis > respiration;

minimum value -3.14 g C m^{-2} d^{-1}). Positive increases in NEP indicative with heterotrophy (i.e., photosynthesis< respiration) occurred later in the year and for longer time periods with increasing depth. Generally, periods of heterotrophy occurred in the winter for 30 m reefs, early summer in the 40 m reefs and throughout the summer and fall in the 60 m reefs (Figures 4B, D, F). Calcification (positive NEC; Figures 4A, C, E) generally occurred between May and December with the greatest rates measured at the 30 m depths and steadily decreased with increased depth (Z = 2.803, p = 0.015; Table 3). The mean NEC (± standard deviation) for the 30 m, 40 m and 60 m reefs for the duration of the study was 10.02 ± 14.32 g CaCO$_3$ m^{-2} d^{-1}, 5.38 ± 9.09 g CaCO$_3$ m^{-2} d^{-1} and 2.81 ± 6.94 g CaCO$_3$ m^{-2} d^{-1} respectively. Whilst the peak monthly average (± standard deviation) calcification periods for all three depth ranges occurred in September (30 m = 36.62 ± 4.23 g CaCO$_3$ m^{-2} d^{-1} in 2017, 40 m = 30.90 ± 0.01 g CaCO$_3$ m^{-2} d^{-1} in 2017) and October (60 m = 16.44 ± 11.74 g CaCO$_3$ m^{-2} d^{-1} in 2018). The highest mean estimate of NEC for the three mesophotic locations was derived from location BT2 (7.38 ± 11.67 g CaCO$_3$ m^{-2} d^{-1}), then location BT3 (4.40 ± 10.11 g CaCO$_3$ m^{-2} d^{-1}). Location BT1 recorded the lowest NEC estimate (2.63 ± 6.03g CaCO$_3$ m^{-2} d^{-1}).

TABLE 2 Summary of physico-chemical parameter averages $\pm$ SE over the duration of the study for the mesophotic coral reef and three reef zones.

Reef zone	Temperature	NEC	NEP	$\Omega_{aragonite}$	$\Omega_{calcite}$	Salinity
	°C	g CaCO$_3$ m^{-2} d^{-1}	g C m^{-2} d^{-1}			g kg^{-1}
Mesophotic	23.09 ± 0.16	4.96 ± 0.74	-0.34 ± 0.07	3.58 ± 0.01	5.44 ± 0.02	36.65 ± 0.01
30 m	24.28 ± 0.25	10.02 ± 2.32	-0.64 ± 0.14	3.59 ± 0.02	5.44 ± 0.03	36.65 ± 0.02
40 m	23.8 ± 0.32	5.38 ± 1.42	-0.35 ± 0.10	3.61 ± 0.02	5.48 ± 0.03	36.67 ± 0.01
60 m	22.33 ± 0.20	2.81 ± 0.70	-0.22 ± 0.10	3.56 ± 0.02	5.42 ± 0.02	36.68 ± 0.01
Reef zone	DIC	TA	NH$_4^+$	NO$_2^-$ + NO$_3^-$	PO$_4^{3-}$	Silicate
	µmoles kg^{-1}	µmoles kg^{-1}	µmoles L^{-1}	µmoles L^{-1}	µmoles L^{-1}	µmoles L^{-1}
Mesophotic	2073 ± 1.25	2398 ± 0.81	0.13 ± 0.05	0.17 ± 0.05	0.01 ± 0.01	0.97 ± 0.04
30 m	2068 ± 2.36	2392 ± 2.18	0.08 ± 0.03	0.27 ± 0.14	0.01 ± 0.01	1.05 ± 0.08
40 m	2070 ± 2.31	2398 ± 1.56	0.05 ± 0.04	0.12 ± 0.05	0.01 ± 0.01	1.01 ± 0.07
60 m	2075 ± 1.79	2401 ± 0.87	0.19 ± 0.09	0.14 ± 0.05	0.01 ± 0.01	0.91 ± 0.05
	NEC calculated using the molecular weight of 100.09			NEP calculated using the molecular weight of 12		

Note, nutrients were collected over the duration of the study at a subset of study locations.

4 Discussion

4.1 Calcification status

Determining how mesophotic reef biogeochemical processes respond to variations of CO_2-carbonate chemistry offers insight to how these understudied ecosystems could respond to future marine environmental conditions. Bermudan mesophotic reefs exhibit both spatial and temporal variability in biogeochemical processes (i.e., the balance of photosynthesis, respiration, calcification, and $CaCO_3$ dissolution). NEC estimates established in this study demonstrate that the seawater chemistry of Bermudan mesophotic reefs are chemically conducive for calcification. The mean NEC for the collective mesophotic reef system and individual reef depths investigated were positive thus indicative of net calcification (Figures 4A, C, E). The greatest rates of NEC were measured at the 30 m depths and steadily decreased with increased depth to a level that the 60 m reefs were in a state of equilibrium (calcification = dissolution) for ~ 6 months of the year. Whilst elevated calcification levels and corresponding draw down of nTA were observed on the 60 m reefs in the latter part of 2017 (September and November), there appeared to be no reduction in $\Omega_{aragonite}$ or pH.

The Bermudan mesophotic benthic community transitions from scleractinian dominated at ~ 30 m to< 1% at 60 m depth range (Goodbody-Gringley et al., 2019). A reduction in NEC with increased depth would be expected due to increased light attenuation and decreased scleractinian percent coral cover with depth. The results support this assumption through a combined reduction in calcification and increase in heterotrophy with increased depth. Observed trends indicate greater estimated rates of NEC associated with higher percent coral cover (Perry et al., 2013; Courtney et al., 2016). Whilst reductions in photosynthesis of corals at ~ 55 – 60 m have been reported to no longer support calcification solely through photosynthetic activity (Mass et al., 2007). The results of this study for the 60 m reefs support the findings of Mass et al. (2007) to a degree. Average

monthly calcification estimated for 60 m reefs were suppressed to near zero for much of the calendar year, however these estimates were irrespective of trophic signal (i.e., photosynthesis or respiration dominated). Exceptions to this trend coincided with the peak calcification period for all three depth ranges which occurred in September and October followed by a period of equilibrium and or dissolution in the winter months. This switch between net accretion and net dissolution has been previously documented on a seasonal basis for Bermudan shallow reefs using the alkalinity anomaly technique (Yeakel et al., 2015; Muehllehner et al., 2016; Bates, 2017; Cyronak et al., 2018; Griffin et al., 2022). The peak calcification periods are in general agreement with a recent study on Bermuda shallow reef calcification (Bates, 2017). The same study also recorded a reduction of accretion rates to near zero during annual cycles over the extent of the 20-year time-series study. The mean NEC rates (Table 2) estimated for the three mesophotic depths (30 m, 40 m, 60 m) were comparable to scaled in situ skeletal growth rates of the Grooved brain coral (*Diploria labryinthiformis* Linnaeus 1758; ~1.30– 3.20 g CaCO$_3$ m^{-2} d^{-1}; Bates et al., 2010) located on the north coral platform of Bermuda at ~10 m depth. However, these skeletal rates should not be taken as a direct comparison since the reef types and environmental conditions are not cognate (Andersson and Gledhill, 2013). Literature on mesophotic biogeochemistry and influences thereof are lacking (Hoegh-Guldberg et al., 2017), therefore it makes it impossible for direct NEC comparisons to other mesophotic locations but to give these values context, they fall within the range of historic Bermudan shallow reef estimates (< 30 m depth; Bates, 2002; Bates et al., 2010; Courtney et al., 2016; Courtney et al., 2017) and average global coral reef NEC values 2.00 – 25.00 g CaCO$_3$ m^{-2} d^{-1} (Atkinson, 2011). Notably, when the mean annual NEC estimates were grouped by either depth range (30 m, 40 m, 60 m) or by location (BT1, BT2, BT3), they were all greater than the mean annual estimate calculated (~2.2 ± 1.6 g CaCO$_3$ m^{-2} d^{-1}) for the shallow Bermuda reef system (Bates, 2017). However, within these groupings there was considerable variation amongst the NEC estimates (e.g., depth; Figure 4). In addition, there was a varying
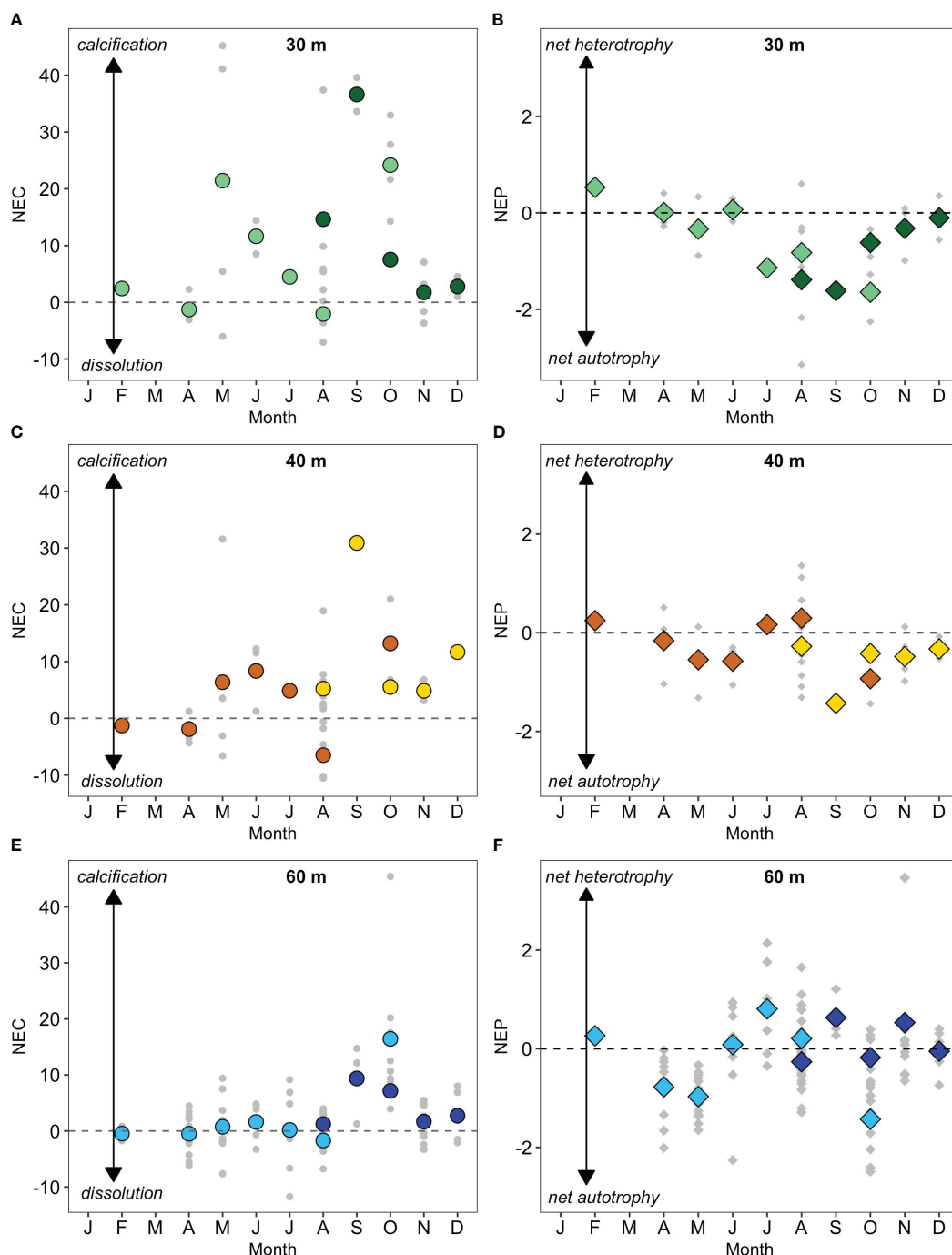
FIGURE 4
Mean seasonal climatology of net ecosystem calcification (NEC; g CaCO$_3$ m^{-2} d^{-1}) and net ecosystem production (NEP; g C m^{-2} d^{-1}) for 30 m, 40m, 60 m reefs. Grey symbols represent actual samples **(A)** NEC, dark green circles denote monthly mean values for 2017, light green circles denote monthly mean values for 2018; **(B)** NEP, dark green diamonds denote monthly mean values for 2017, light green diamonds circles denote monthly mean values for 2018; **(C)** NEC, orange circles denote monthly mean values for 2017, dark orange circles denote monthly mean values for 2018; **(D)** NEP, orange diamonds denote monthly mean values for 2017, dark orange diamonds denote monthly mean values for 2018; **(E)** NEC, dark blue circles denote monthly mean values for 2017, light blue circles denote monthly mean values for 2018; **(F)** NEP, dark blue diamond's denote monthly mean values for 2017, light blue diamond's denote monthly mean values for 2018. Dashed lines equal calcification and trophic status are in balance (e.g., NEC = 0, NEP = 0).

duration of the accumulative amount of time the three independent 60 m locations spent in a state of net calcification during the study period (BT1 = 69%, BT2 = 76%, BT3 = 66%). The differences of NEC estimates across both depth and location suggest mesophotic reefs to be

dynamic environments and likely reflect a complex interplay between abiotic factors and hydrology (Williams et al., 2018). This was evident though coterminous 15-minute temperature measurements that recorded ~2– 4°C daily temperature fluctuations (Figure 5) at the

TABLE 3 Summary of analyses statistically comparing Net Ecosystem Calcification (NEC) and Net Ecosystem Production (NEP) between sampling depth (m) and time of year (Kruskal-Wallis H test).

NEC	Kruskal-Wallis H			NEC	Dunn's test	
					(Kruskal-Wallis multiple comparison)	
	df	*H*	*P*		*Z*	*P.adj*
Depth	2	9.013	**0.011**	Depth		
				30 m – 40 m	0.862	0.388
				30 m – 60 m	2.803	**0.015**
				40 m – 60 m	1.835	0.100
Season	3	35.686	**<0.001**	Season		
				Autumn – Spring	5.320	**<0.001**
				Autumn – Summer	4.892	**<0.001**
				Spring – Summer	-1.213	0.270
				Autumn – Winter	2.096	0.072
				Spring – Winter	-1.691	0.136
				Summer – Winter	-0.949	0.342
NEP	**Kruskal-Wallis H**			**NEP**	**Dunn's test**	
					(Kruskal-Wallis multiple comparison)	
	df	*H*	*P*		*Z*	*P.adj*
Depth	2	3.728	0.155	Depth		
				30 m – 40 m	-0.945	0.517
				30 m – 60 m	-1.910	0.168
				40 m – 60 m	-0.818	0.413
Season	3	17.144	**<0.001**	Season		
				Autumn – Spring	0.338	0.735
				Autumn – Summer	-2.931	**0.010**
				Spring – Summer	-2.939	**0.020**
				Autumn – Winter	-2.750	**0.009**
				Spring – Winter	-2.846	**0.009**
				Summer – Winter	-0.956	0.407

Variation in community NEC and NEP between sampling depth (m) and time of year (Dunn's test).
Bold values equal adjusted p values ≤ 0.01.

central 60 m site at each of the three study locations. Whilst these measurements do not encompass the full study period, they are in agreement with trends observed in both Caribbean (Leichter and Genovese, 2006) and Pacific mesophotic reefs (Wolanski et al., 2004; Colin, 2009; Colin and Lindfield, 2019) where temperature variability has been attributed to internal waves.

Vertical oscillations of the thermocline provide potential pathways for enhancement (e.g., calcification and respiration) on mesophotic reefs. Bates (2017) and a separate study by Yeakel et al. (2015) suggested episodic events of elevated NEC indicative of high calcification could be enhanced through alternative carbon sources (i.e., acquisition of organic nutrients through advection of biomass, e.g., zooplankton) as indicated by increased heterotrophy (> NEP;

Figures 4E, F). This potential response appears to be evident in elevated measurements of NEP from the 60 m reefs in September and November 2017. Yeakel et al. (2015) postulate these changes in metabolite source led to elevated summertime calcification rates (NEC), draw down of nTA and a reduction in pH and $\Omega_{aragonite}$. These high calcification/acidification events were correlated with a negative winter North Atlantic Oscillation (NAO). Whilst autotrophy (photosynthesis by symbiont) is the primary energy source for most scleractinian corals, it has been demonstrated that up to ~ 60% of the metabolic requirements of a coral (Houlbrèque and Ferrier-Pagès, 2009) can be supplied through heterotrophy (i.e., incorporation of particulate and dissolved organic matter, respiration). Mesocosm based feeding experiments have shown this input of organic carbon can
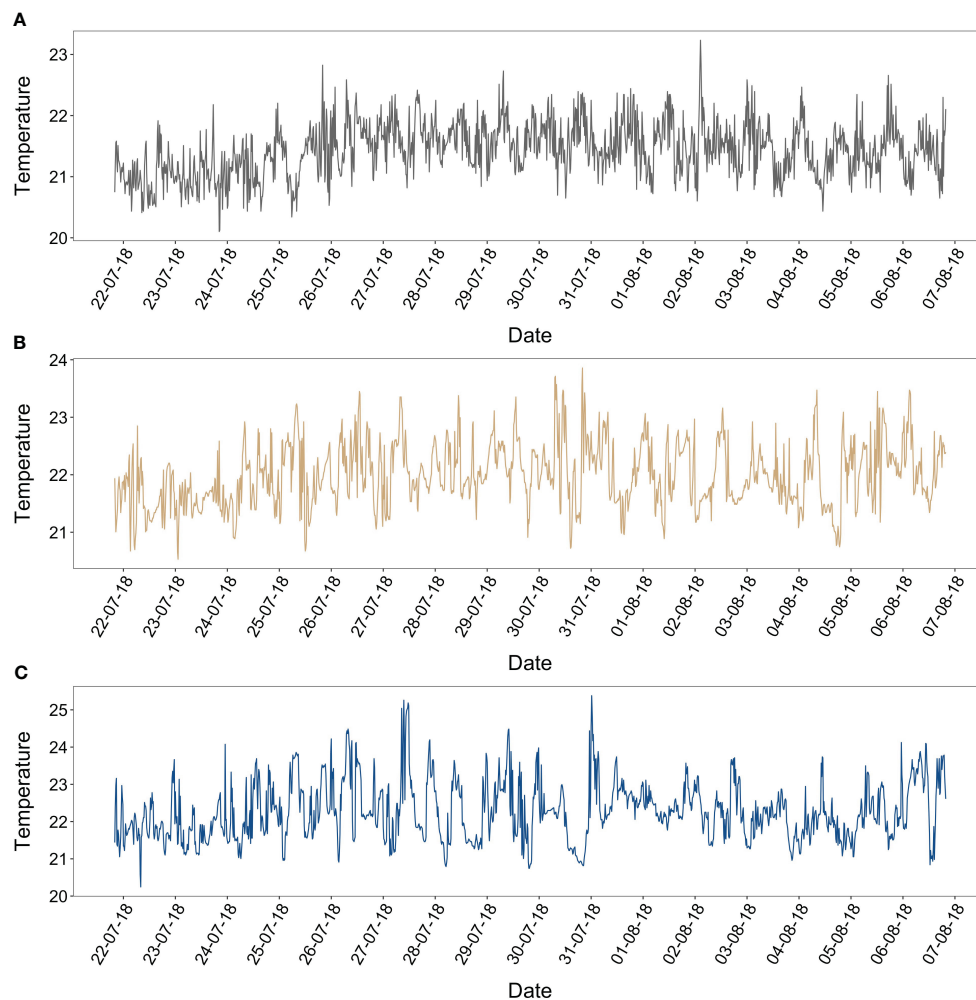
FIGURE 5
Fifteen-minute temperature °C intervals records (22nd July – 6th August 2018) at 60 m depths. **(A)** BT1 (dark grey line), **(B)** BT2 (peril line), **(C)** BT3 (blue line).

maintain calcification rates under ocean acidification conditions (Drenkard et al., 2013; Towle et al., 2015) as well as enhance photosynthesis (Houlbrèque and Ferrier-Pagès, 2009). A study by Leichter and Genovese (2006) recorded bimodal growth patterns of the branching pencil coral (*Madracis auretenra* Locke et al., 2007) at mesophotic depths (30– 55 m) from Florida and Jamacia that were attributed to vertical oscillations of the thermocline providing alternative resources (i.e., heterotrophic particle capture). The same study attributed the higher growth rates of pencil coral recorded at the Florida study location to a greater level of internal wave activity. Increases in both phytoplankton and zooplankton biomass have been documented at the BATS site (~ 80 km southeast of Bermuda), with resultant increases in suspended particulate organic matter by ~ 30% per decade since the initiation of BATS in 1988 (Bates and Johnson, 2021). One could hypothesize that through geographical location, mesophotic reefs, at least for Bermuda, are the "boundary layer" between the open ocean and shallow reefs. One would surmise that any benefits episodic events such as the winter NAO afford shallow corals through advection of biomass onto the reef, would happen on a more frequent basis for mesophotic reefs (Leichter et al., 1996).

Internal waves are generally associated with drawing in cooler subthermocline water onto reef slopes (Leichter and Genovese, 2006; Wyatt et al., 2020; Diaz et al., 2023). However, recent results have demonstrated the opposite can occur, with advection of warmer surface waters down to mesophotic depths (Wyatt et al., 2020; Diaz et al., 2023). Warmer seawater temperatures can facilitate higher calcification rates until a thermal threshold is reached (Bove et al., 2020), levels of which can be dictated by various factors such as species and latitude (Cooper et al., 2012). A recent study of the thermal tolerance of four scleractinian corals common to Bermuda's mesophotic reefs (Gould et al., 2021), determined there to be similar sensitives to adjacent shallow water conspecifics (i.e., similar bleaching thresholds). Therefore, the scleractinian contingent of Bermuda's mesophotic reefs (i.e., high-latitude reefs) can tolerate increases in in situ temperatures through internal waves and potentially benefit from thermally enhanced calcification albeit to the point of reaching a thermal threshold. Thermal enhancement of cooler high-latitude shallow reefs (< 30 m) has recently been documented at the Flower Garden Banks in the Gulf of Mexico (Manzello et al., 2021). One should note that the thermal trends recorded ~ 80 km from Bermuda's

high-latitude reefs show an extension of the summer period for water ≥ 25°C by approximately a month (Bates and Johnson, 2020) with average temperatures of the upper 500 m increasing by 1.4°C within the last 50 years (Bates and Johnson, 2021). The combination of thermal variability, an increase in the summer period and potential advection of alternative carbon resources, would explain the disparities between NEC estimates presented in this study and the mean annual NEC estimate for adjacent shallow reefs (Bates, 2017).

4.2 Trophic status

The trophic response of mesophotic reefs were similar when the study sites were partitioned by location (i.e., BT1, BT2, BT3) The three locations were all accumulatively in a state of net heterotrophy for ~ 30% of the study period. The same trend was not observed when partitioned by depth range. Greater depth corresponded with a reduction in autotrophy and a stronger signal of heterotrophy (photosynthesis< respiration), as would be expected due to factors such as light attenuation limiting photosynthesis.

The monthly mean NEP estimates for the 30 m reefs between February and June fluctuated between a balanced state whereby NEP was close to zero prior to switching to net autotrophy for the remainder of the year (photosynthesis > respiration). During this same timeframe, the 40 m reef systems switched to a state of net autotrophy during May and June. The 60 m reefs were generally in a state of equilibrium or net autotrophy during this period followed by positive NEP indicative with heterotrophy (i.e., photosynthesis< respiration) or equilibrium between June – February. This pattern of net autotrophy in the early summer with a shift to strong heterotrophy in late summer was described by Bates et al. (2010) as the "Carbonate Chemistry Coral Reef Ecosystem Feedback" (CREF hypothesis). During the summer months, elevated autotrophy (e.g., scleractinian coral calcifying) heighten the $\Omega_{aragonite}$, and $[CO_3^{2-}]$ conditions (e.g., CO_2 uptake and photosynthesis). In the late summer (October; Bates et al., 2010), there is a switch in metabolic source, CO_2 released through respiration leads to a suppression of photosynthetic activity. Evidence for this can be seen in Figures 4B, D, F albeit the estimated NEP values do not become positive (i.e., heterotrophic) for either the 30 m or 40 m reefs. Instead, the feedback causes a strong reduction in autotrophy closer to a state of equilibrium. Whilst there was variability between the three reef depths, the overall status of the mesophotic system was net autotrophic (-0.34 ± 0.92 g C m^{-2} d^{-1}) and not in a state of balance. This determination is the opposite of the trophic evaluation for Bermuda shallow reefs (net heterotrophic; + 0.20 ± 0.9 g C m^{-2} d^{-1}). These findings present an interesting conundrum. Zooxanthellate corals are generally restricted to depths where light levels typically exceed the 0.5% of the subsurface intensity (Dubinsky and Stambler, 2011). Therefore, light availability is a primary factor that drives the vertical zonation of communities. The classical viewpoint would be to expect that the shallow water reefs would be more likely to derive carbon by way of the inorganic carbon cycle (i.e., photosynthesis) due to greater levels of surface irradiance. However, as discussed in the calcification section, there are energetic benefits when zooxanthellate corals utilize both inorganic and organic carbon sources (photosynthesis + respiration). It does raise the question about the exact composition of the primary calcifiers at mesophotic depths and how representative are these rate measurements and if we truly are "taking the metabolic pulse" of these communities (Cyronak et al., 2018).

4.3 Other considerations

Scleractinian (stony) corals are considered dominant calcifiers on reef systems however, knowledge on benthic community composition for mesophotic reefs is lacking on a global scale (Loya et al., 2019). Goodbody-Gringley et al. (2019) summarize known information for Bermuda and a recent field guide to Bermuda's MCEs has been produced (Stefanoudis et al., 2018). Based on a limited number of quantitative surveys (n = 5) algae and a sand/rubble complex account for 69% and ~25% of the broad functional groupings of the benthic community at 60 m depths respectively. For context, Scleractinia represent 0.02% of these data. To further complicate our understanding of these complex biogeochemical processes, there are alternative inputs of $CaCO_3$ and alkalinity fluxes that have not yet been considered. All marine teleosts produce and excrete $CaCO_3$ as an osmoregulatory product due to the constant swallowing of seawater (Wilson et al., 2009). Calcium carbonate precipitates into the digestive tract and is excreted either as pellets or with fecal matter which has been estimated to contribute ~ 3 – 15% of total new $CaCO_3$ production to the upper oceanic environment (Wilson et al., 2009). Dissolution of the excreted $CaCO_3$ would lead to increases in total alkalinity. It should be noted that the calculated NEC rates are a relative expression of the balance of calcification and dissolution based on observed differences between offshore and in situ normalized TA measurements (Equation 4). Increases in offshore TA values would result in a stronger positive NEC signal. Alternatively, increases in mesophotic TA values would correspond to a stronger negative NEC signal (net accretion< net dissolution). Hypothetically, fluctuations in fish abundances at either mesophotic or reference sites (e.g., diel vertical migration of deep-sea fish) could lead to direct changes in biogeochemical processes and alternative interpretation of calcification/dissolution results. To give context for Bermudan mesophotic fish communities, evaluations have determined there to be increases in species richness, abundance and biomass with depth, an apparent apposing pattern to Caribbean MCE communities (Pinheiro et al., 2016).

Additionally, within the algal grouping, encrusting crustose coralline algae (CCA) and rhodoliths are the main calcifying taxa. Rhodoliths and CCA perform valuable ecosystem services of substrate provision through calcification. Which carbonate mineral phase (i.e., aragonite, calcite, and magnesian calcite– Mg-calcite) these red algae utilize for calcification is taxa specific (Nash et al., 2019) but in the case of *Corallinales*, the carbonate mineral phase is Mg-calcite (Nash et al., 2011). Gorgonians are known to calcify using Mg-calcite (Bond et al., 2005) and are common constituents of MCEs having recently been described as foundation species for mesophotic reefs within the Caribbean Basin (Slattery and Lesser, 2021). A study on the effects of ocean acidification on *Corallium rubrum* (Linnaeus, 1758) demonstrated lower pH (7.81 pH) significantly reduced skeletal growth (Bramanti

et al., 2013), therefore till disproven, one could assume a similar response by *Corallinales* and octocorals (Goodbody-Gringley et al., 2019) documented on Bermudan MCEs.

The effect of ocean acidification (OA) and the reduction of seawater saturation state on marine organisms' ability to accrete $CaCO_3$ has been well documented in the literature. However, studies do not tend to delineate between different carbonate mineral phase (i.e., aragonite, calcite, and Mg-calcite) saturation states (Lebrato et al., 2016) often referring to fluctuations in $\Omega_{aragonite}$ or $\Omega_{calcite}$. Magnesium calcite minerals that have a magnesium content greater than 8 – 12 mol% are more soluble than both aragonite and calcite (Gattuso and Hansson, 2011). New evidence suggests $\Omega_{aragonite}$ or $\Omega_{calcite}$ do not account for the Mg content of calcite (increased solubility) therefore are not appropriate estimates of seawater saturation state with respect to Mg-calcite (Lebrato et al., 2016). The same study determined that 24% of benthic calcite producing calcifiers are currently experiencing under saturated conditions (i.e., dissolution; $\Omega_{Mgcalcite-x}$) with the majority (95%) of those calcifiers occurring in the tropics.

Griffin et al. (2022) demonstrated the combined use of the TA anomaly technique with measurements of dissolved calcium (Ca) to salinity (S) ratio (Chisholm and Gattuso, 1991) relative to reference values. The Ca method is an alternative approach for estimating NEC that is strongly influenced by $CaCO_3$ precipitation and dissolution, albeit with analytical challenges that has led to the TA anomaly technique being the dominant method for estimating coral reef NEC (Griffin et al., 2022). Analytical challenges aside, the use of the Ca NEC approach could allow for the identification of the relative contribution (i.e., importance) of different mineral phases (i.e., $Mg_xCa_{1-x}CO_3$); relative to calcite and aragonite through direct comparisons of rates derived by the TA anomaly technique (Andersson et al., 2007). This in turn would allow for more robust mesophotic NEC estimates and a greater understanding of the relative contribution of different calcifying groups (e.g., stony corals, CCA or gorgonians) to NEC rates and therefore responses under varying CO_2-carbonate chemistry conditions.

A lack of long-term measurements restricts our ability to fully interpret natural and seasonal variability of mesophotic biogeochemistry. Ultimately, this hinders our capacity to predict biogeochemical responses of these environments to future OA and climate change scenarios. The predicted effects of OA on calcifying benthic communities are often based on the relationship between average $\Omega_{aragonite}$ and NEC (gross calcification – gross $CaCO_3$ dissolution) which typically changes at a rate of 102% NEC per unit change of seawater $\Omega_{aragonite}$ (Eyre et al., 2018). However, site-specific disparities between $\Omega_{aragonite}$ and NEC that are likely a reflection of benthic community composition (Eyre et al., 2018) and the variability between individual benthic communities (i.e., corals, gorgonians, CCA), have been observed (Page et al., 2017; Davis et al., 2019). Recent meta-analysis of ecosystem-scale chemistry-based NEC derived estimates revealed calcification was primarily driven by depth and benthic calcifier cover (Davis et al., 2021) suggesting $\Omega_{aragonite}$ may not be as useful for predicting long-term NEC estimates as previously thought. Davis et al. (2021) did highlight an under representation of reef NEC estimates for certain locations and latitudes however,

mesophotic reefs were not specifically recognized as fitting this definition. It should be recognized that the estimated rates of NEC are of the balance between calcification and $CaCO_3$ dissolution. As such, they might not be directly coupled to benthic calcification but also reflect changes in sediment transport or bioerosion. (i.e., NEC increases due to reduction in sediment transport).

The hydrodynamic regime of mesophotic reefs can drive ecosystem calcification through the links with seawater temperature variability (i.e., internal waves), flow rates and direction, advection of alternative carbon sources (e.g., sediment transport) and indirectly through the equations utilized to calculated NEC (i.e., residence times; Courtney and Andersson, 2019). Page et al. (2017) postulated that insufficient characterization of flow rates and residence times greatly influenced NEC estimates generated from mesocosm experiments. Due to a lack of empirical data, in situ seawater residence times for mesophotic sites were derived from hydrological modelling. However, the generation of quantitative data, for example through the deployment of Acoustic Doppler Current Profilers (ADCPs) would allow for greater characterization of localized fine-scale hydrodynamics and therefore potential influences over ecosystem calcification.

5 Conclusions

The estimates of NEC and NEP derived by this 15-month investigation represent the first known biogeochemical measurements for mesophotic reefs and therefore provide the critical first step towards enabling our predictive capabilities on their future status. The measured seawater CO_2-carbonate chemistry from these reef ecosystems were chemically conducive for calcification. The unique location of the study allows these measurements to be considered in the context of high-latitude reefs with contemporaneous offshore changes observed at the longest-running time-series for biogeochemical oceanographic data (BATS). All three mesophotic reef zones were net accretive (i.e., gross calcification > gross $CaCO_3$ dissolution) and in a net state of autotrophy whilst exhibiting signs of increased NEC in the summer and reduced NEC in the winter. In addition, these systems exhibited periods of variability through a trophic switch between autotrophy and heterotrophy that was influenced by depth. It remains to be determined why the mesophotic reefs are in opposing trophic states to those of the shallow reef counter parts (MCE = net autotrophic, shallow reefs = net heterotrophic; Bates, 2017). Although the values established by this study demonstrate just how close these understudied ecosystems are in terms of the known boundary thresholds for low saturation states of reefs. The apparent increase in NEC and NEP rates (~30%) on Bermudan shallow reefs over the last 20 years (Bates, 2017) are an indication that there is a level of resilience to the changing environment that may extend to MCEs. At what level and for how long are critical questions that will need to be urgently addressed in the near future.

Data availability statement

The raw data supporting the conclusions of this article will be made available by the authors, without undue reservation.

Author contributions

Funding

Acknowledgments

Conflict of interest

The authors declare that the research was conducted in the absence of any commercial or financial relationships that could be construed as a potential conflict of interest.

Publisher's note

References

Andersson, A. J., Bates, N. R., and Mackenzie, F. T. (2007). Dissolution of carbonate sediments under rising pCO2 and ocean acidification: Observations from Devil's Hole, Bermuda. *Aquat Geochem* 13, 237–264. doi: 10.1007/s10498-007-9018-8

Andersson, A. J., and Gledhill, D. (2013). Ocean acidification and coral reefs: effects on breakdown, dissolution, and net ecosystem calcification. *Ann. Rev. Mar. Sci.* 5, 321–348. doi: 10.1146/annurev-marine-121211-172241

Andersson, A. J., Kuffner, I. B., MacKenzie, F. T., Jokiel, P. L., Rodgers, K. S., and Tan, A. (2009). Net Loss of CaCO3 from a subtropical calcifying community due to seawater acidification: Mesocosm-scale experimental evidence. *Biogeosciences* 6, 1811–1823. doi: 10.5194/bg-6-1811-2009

Andersson, A. J., Yeakel, K. L., Bates, N. R., and De Putron, S. J. (2014). Partial offsets in ocean acidification from changing coral reef biogeochemistry. *Nat. Clim. Chang.* 4, 56–61. doi: 10.1038/nclimate2050

Atkinson, M. J. (2011). "Biogeochemistry of nutrients," in *Coral reefs: An ecosystem in transition*. Eds. Z. Dubinsky and S. Stambler (Dordrecht: Springer Netherlands), 199–206. doi: 10.1007/978-94-007-0114-4_13

Baker, E., Puglise, K., and Harris, P. (2016). *Mesophotic Coral Ecosystems - A Lifeboat for Coral Reefs?* (Nairobi and Arendal: The United Nations Environment Programme and GRID-Arendal).

Bates, N. R. (2002). Seasonal variability of the effect of coral reefs on seawater CO 2 and air-sea CO 2 exchange. *Limnol. Oceanogr.* 47, 43–52. doi: 10.4319/lo.2002.47.1.0043

Bates, N. R. (2017). Twenty years of marine carbon cycle observations at Devils Hole Bermuda provide insights into seasonal hypoxia, coral reef calcification, and ocean acidification. *Front. Mar. Sci.* 4. doi: 10.3389/fmars.2017.00036

Bates, N. R., Amat, A., and Andersson, A. J. (2010). Feedbacks and responses of coral calcification on the Bermuda reef system to seasonal changes in biological processes and ocean acidification. *Biogeosciences* 7, 2509–2530. doi: 10.5194/bg-7-2509-2010

Bates, N. R., Best, M. H. P., Neely, K., Garley, R., Dickson, A. G., and Johnson, R. J. (2012). Detecting anthropogenic carbon dioxide uptake and ocean acidification in the North Atlantic Ocean. *Biogeosciences* 9, 2509–2522. doi: 10.5194/bg-9-2509-2012

Bates, N. R., and Johnson, R. J. (2020). Acceleration of ocean warming, salinification, deoxygenation and acidification in the surface subtropical North Atlantic Ocean. *Commun. Earth Environ.* 1. doi: 10.1038/s43247-020-00030-5

Bates, N. R., and Johnson, R. J. (2021). Ocean observing in the North Atlantic subtropical gyre. *Oceanography* 4, 32–33. doi: 10.5670/oceanog.2021.supplement.02-14

Bates, N. R., Michaels, A. F., and Knap, A. H. (1996). Alkalinity changes in the Sargasso Sea: of calcification? *Mar. Chem.* 51, 347–358. doi: 10.1016/0304-4203(95)00068-2

Bond, Z. A., Cohen, A. L., Smith, S. R., and Jenkins, W. J. (2005). Growth and composition of high-Mg calcite in the skeleton of a Bermudian gorgonian (Plexaurella dichotoma): Potential for paleothermometry. *Geochem. Geophys. Geosys.* 6, 1–10. doi: 10.1029/2005GC000911

Bongaerts, P., Muir, P., Englebert, N., Bridge, T. C. L., and Hoegh-Guldberg, O. (2013). Cyclone damage at mesophotic depths on Myrmidon Reef (GBR). *Coral Reefs* 32, 935. doi: 10.1007/s00338-013-1052-y

Bongaerts, P., Ridgway, T., Sampayo, E. M., and Hoegh-Guldberg, O. (2010). Assessing the "deep reef refugia" hypothesis: Focus on Caribbean reefs. *Coral Reefs* 29, 1–19. doi: 10.1007/s00338-009-0581-x

Bongaerts, P., Riginos, C., Brunner, R., Englebert, N., Smith, S. R., and Hoegh-Guldberg, O. (2017). Deep reefs are not universal refuges: Reseeding potential varies among coral species. *Sci. Adv.* 3, 1–12. doi: 10.1126/sciadv.1602373

Bove, C. B., Umbanhowar, J., and Castillo, K. D. (2020). Meta-analysis reveals reduced coral calcification under projected ocean warming but not under acidification across the caribbean sea. *Front. Mar. Sci.* 7. doi: 10.3389/fmars.2020.00127

Bramanti, L., Movilla, J., Guron, M., Calvo, E., Gori, A., Dominguez-Carrió, C., et al (2013). Detrimental effects of ocean acidification on the economically important Mediterranean red coral (Corallium rubrum). *Glob. Chang. Biol.* 19, 1897–1908. doi: 10.1111/gcb.12171

Bridge, T. C. L., Hughes, T. P., Guinotte, J. M., and Bongaerts, P. (2013). Call to protect all coral reefs. *Nat. Clim. Chang.* 3, 528–530. doi: 10.1038/nclimate1879

Chisholm, J. R. M., and Gattuso, J. P. (1991). Validation of the alkalinity anomaly technique for investigating calcification of photosynthesis in coral reef communities. *Limnol. Oceanogr.* 36, 1232–1239. doi: 10.4319/lo.1991.36.6.1232

Cinner, J. E., Huchery, C., MacNeil, M. A., Graham, N. A. J., McClanahan, T. R., Maina, J., et al. (2016). Bright spots among the world's coral reefs. *Nature* 535, 416–419. doi: 10.1038/nature18607

Coates, K. A., Fourqurean, J. W., Kenworthy, W. J., Logan, A., Manuel, S. A., and Smith, S. R. (2013), 115–133. doi: 10.1007/978-94-007-5965-7_10

Cohen, A. (2003). Geochemical perspectives on coral mineralization. *Rev. Mineral Geochem* 54, 151–187. doi: 10.2113/0540151

Colin, P. L. (2009). *Marine environments of Palau* (San Diego: Indo-Pacific Press).

Colin, P. L., and Lindfield, S. J. (2019). "Palau," in *Mesophotic Coral Ecosystems Coral Reefs of the World 12*. Eds. Y. Loya, K. Puglise and T. C. L. Bridge (Cham: Springer), 285–320. doi: 10.1007/978-3-319-9275-0_16

Cooper, T. F., O'Leary, R. A., and Lough, J. M. (2012). Growth of western Australian corals in the anthropocene. *Sci. (1979)* 335, 593–596. doi: 10.1126/science.1214570

Courtney, T. A., and Andersson, A. J. (2019). Evaluating measurements of coral reef net ecosystem calcification rates. *Coral Reefs* 38, 997–1006. doi: 10.1007/s00338-019-01828-2

Courtney, T. A., Andersson, A. J., Bates, N. R., Collins, A., Cyronak, T., de Putron, S. J., et al. (2016). Comparing chemistry and census-based estimates of net ecosystem calcification on a rim reef in Bermuda. *Front. Mar. Sci.* 3, 1–9. doi: 10.3389/fmars.2016.00181

Courtney, T. A., Cyronak, T., Griffin, A. J., and Andersson, A. J. (2021). Implications of salinity normalization of seawater total alkalinity in coral reef metabolism studies. *PloS One* 16, 1–13. doi: 10.1371/journal.pone.0261210

Courtney, T. A., Lebrato, M., Bates, N. R., Collins, A., De Putron, S. J., Garley, R., et al. (2017). Environmental controls on modern scleractinian coral and reef-scale calcification. *Sci. Adv.* 3, 1–17. doi: 10.1126/sciadv.1701356

Cyronak, T., Andersson, A. J., Langdon, C., Albright, R., Bates, N. R., Caldeira, K., et al. (2018). Taking the metabolic pulse of the world's coral reefs. *PloS One* 13, 105. doi: 10.1371/journal.pone.0190872

Davis, K. L., Colefax, A. P., Tucker, J. P., Kelaher, B. P., and Santos, I. R. (2021). Global coral reef ecosystems exhibit declining calcification and increasing primary productivity. *Commun. Earth Environ.* 2, 6528. doi: 10.1038/s43247-021-00168-w

Davis, K. L., McMahon, A., Kelaher, B., Shaw, E., and Santos, I. R. (2019). Fifty years of sporadic coral reef calcification estimates at One Tree Island, Great Barrier Reef: Is it enough to imply long term trends? *Front. Mar. Sci.* 6. doi: 10.3389/fmars.2019.00282

Diaz, C., Foster, N. L., Attrill, M. J., Bolton, A., Ganderton, P., Howell, K. L., et al. (2023). Mesophotic coral bleaching associated with changes in thermocline depth. *Nat. Commun.* 14. doi: 10.1038/s41467-023-42279-2

Dickson, A. G., and Millero, F. J. (1987). A comparison of the equilibrium constants for the dissociation of carbonic acid in seawater media. *Deep Sea Res. Part A Oceanographic Res. Papers* 34, 1733–1743. doi: 10.1016/0198-0149(87)90021-5

Dickson, A. G., Sabine, C. L., and Christian, J. R. (2007). *Guide to Best Practices for Ocean CO2 measurements* (North Pacific Marine Science Organization).

Dove, S. G., Kline, D. I., Pantos, O., Angly, F. E., Tyson, G. W., and Hoegh-Guldberg, O. (2013). Future reef decalcification under a business-as-usual CO2 emission scenario. *Proc. Natl. Acad. Sci. U.S.A.* 110, 15342–15347. doi: 10.1073/pnas.1302701110

Drenkard, E. J., Cohen, A. L., McCorkle, D. C., de Putron, S. J., Starczak, V. R., and Zicht, A. E. (2013). Calcification by juvenile corals under heterotrophy and elevated CO2. *Coral Reefs* 32, 727–735. doi: 10.1007/s00338-013-1021-5

Dubinsky, Z., and Stambler, N. (2011). Coral reefs: An ecosystem in transition. *Coral Reefs: Ecosystem Transition*. Eds. Z. Dubinsky and S. Stambler (Dordrecht: Springer Netherlands), 1–552. doi: 10.1007/978-94-007-0114-4

Eyre, B. D., Cyronak, T., Drupp, P., De Carlo, E. H., Sachs, J. P., and Andersson, A. J. (2018). Coral reefs will transition to net dissolving before end of century. *Sci. (1979)* 359, 908–911. doi: 10.1126/science.aao1118

Fricke, H., and Meischner, D. (1985). Depth limits of Bermudan scleractinian corals: a submersible survey. *Mar. Biol.* 88, 175–187.

Gattuso, J.-P., and Hansson, L. eds. (2011). *Ocean Acidification* (Oxford University Press). doi: 10.1093/oso/9780199591091.001.0001

Gattuso, J.-P., Pichon, M., Delesalle, B., Canon, C., and Frankignoulle, M. (1996). Carbon fluxes in coral reefs. I. Lagrangian measurement of community metabolism and resulting air-sea CO2 disequilibrium. *Mar. Ecol. Prog. Ser.* 145, 109–121. doi: 10.3354/meps145109

Glynn, P. W. (1996). Coral reef bleaching: Facts, hypotheses and implications. *Glob. Chang. Biol.* 2, 495–509. doi: 10.1111/j.1365-2486.1996.tb00063.x

Goodbody-Gringley, G., Marchini, C., Chequer, A. D., and Goffredo, S. (2015). Population structure of Montastraea cavernosa on shallow versus mesophotic reefs in Bermuda. *PloS One* 10, e0142427. doi: 10.1371/journal.pone.0142427

Goodbody-Gringley, G., Noyes, T., and Smith, S. R. (2019). "Bermuda," in *Mesophotic Coral Ecosystems, Coral Reefs of the World 12*. Eds. L. Yossi, K. A. Puglise and T. Bridge (Cham: Springer), 31–45. doi: 10.1007/978-3-319-92735-0_2

Gould, K., Bruno, J. F., Ju, R., and Goodbody-gringley, G. (2021). Upper-mesophotic and shallow reef corals exhibit similar thermal tolerance, sensitivity and optima. *Coral Reefs*. 40, 907–920. doi: 10.1007/s00338-021-02095-w

Griffin, A. J., Anderson, Z., Ballard, J., Bates, N. R., Garley, R., Johnson, R., et al. (2022). Seasonal changes in seawater calcium and alkalinity in the Sargasso Sea and across the Bermuda carbonate platform. *Mar. Chem.* 238, 104064. doi: 10.1016/j.marchem.2021.104064

Hinderstein, L. M., Marr, J. C. A., Martinez, F. A., Dowgiallo, M. J., Puglise, K. A., Pyle, R. L., et al. (2010). Theme section on "Mesophotic coral ecosystems: characterization, ecology, and management." *Coral Reefs* 29, 247–251. doi: 10.1007/s00338-010-0614-5

Hoegh-Guldberg, O. (2011). Coral reef ecosystems and anthropogenic climate change. *Reg. Environ. Change* 11, 215–227. doi: 10.1007/s10113-010-0189-2

Hoegh-Guldberg, O., Mumby, P. J., Hooten, A. J., Steneck, R. S., Greenfield, P., Gomez, E., et al. (2007). Coral reefs under rapid climate change and ocean acidification. *Sci. (1979)* 318, 1737–1742. doi: 10.1126/science.1152509

Hoegh-Guldberg, O., Poloczanska, E. S., Skirving, W., and Dove, S. (2017). Coral reef ecosystems under climate change and ocean acidification. *Front. Mar. Sci.* 4. doi: 10.3389/fmars.2017.00158

Houlbrèque, F., and Ferrier-Pagès, C. (2009). Heterotrophy in tropical scleractinian corals. *Biol. Rev.* 84, 1–17. doi: 10.1111/j.1469-185X.2008.00058.x

Hughes, T. P., Rodrigues, M. J., Bellwood, D. R., Ceccarelli, D., Hoegh-Guldberg, O., McCook, L., et al. (2007). Phase shifts, herbivory, and the resilience of coral reefs to climate change. *Curr. Biol.* 17, 360–365. doi: 10.1016/j.cub.2006.12.049

J. Jackson, M. Donovan, K. Cramer and V. Lam (Eds.) (2014). *Status and Trends of Caribbean Coral Reefs: 1970-2012* (Gland, Switzerland: Global Coral Reef Monitoring Network, IUCN). doi: 10.1016/0377-8401(86)90099-4

Jackson, J. B. C., Kirby, M. X., Berger, W. H., Bjorndal, K. A., Botsford, L. W., Bourque, B. J., et al. (2001). Historical overfishing and the recent collapse of coastal ecosystems. *Sci. (1979)* 293, 629–637. doi: 10.1126/science.1059199

Jones, R., Johnson, R., Noyes, T., and Parsons, R. (2012). Spatial and temporal patterns of coral black band disease in relation to a major sewage outfall. *Mar. Ecol. Prog. Ser.* 462, 79–92. doi: 10.3354/meps09815

Kinsey, D. W. (1978). Alkalinity changes and coral reef calcification. *Limnol. Oceanogr.* 23, 989–991. doi: 10.4319/lo.1978.23.5.0989

Kleypas, J. A., Buddemeier, R. W., Archer, D., Gattuso, J. P., Langdon, C., and Opdyke, B. N. (1999). Geochemical consequences of increased atmospheric carbon dioxide on coral reefs. *Sci. (1979)* 284, 118–120. doi: 10.1126/science.284.5411.118

Kleypas, J. A., Buddemeier, R. W., and Gattuso, J. P. (2001). The future of Coral reefs in an age of global change. *Int. J. Earth Sci.* 90, 426–437. doi: 10.1007/s005310000125

Knap, A., Michaels, A. F., Steinberg, D. K. D., Bahr, F., Bates, N., Bell, S., et al. (1997). "BATS methods manual," in *Version 4* (Woods Hole: U.S. JGOFS Planning Office).

Ku, H. H. (1966). Notes on the use of propagation of error formulas. Journal of Research of the National Bureau of Standards. *Section C: Engineering and Instrumentation* 70C, 263. doi: 10.6028/jres.070C.025

Langdon, C., Gattuso, J.-P., and Andersson, A. (2010). "Measurements of calcification and dissolution of benthic organisms and communities," in *Guide to beast practices for ocean acidification research and data reporting*. Eds. U. Riebesell, V. Fabry, L. Hansson and J.-P. Gattuso (Luxembourg: Publications of the European Union), 213–232.

Langdon, C., Takahashi, T., Sweeney, C., Chipman, D., and Atkinson, J. (2000). rate of an experimental coral reef responds to manipulations in the concentrations of both Ca CO •. *Global Biogeochem. Cycles* 14, 639–654. doi: 10.1029/1999GB001195

Lantz, C. A., Atkinson, M. J., Winn, C. W., and Kahng, S. E. (2014). Dissolved inorganic carbon and total alkalinity of a Hawaiian fringing reef: Chemical techniques for monitoring the effects of ocean acidification on coral reefs. *Coral Reefs* 33, 105–115. doi: 10.1007/s00338-013-1082-5

Lebrato, M., Andersson, A., Ries, J., Aronson, R., Lamare, M., Koeve, W., et al. (2016). Benthic marine calcifiers coexist with CaCO3 undersaturated seawater worldwide. *Global Biogeochem Cycles* 30, 1–16. doi: 10.1002/2015GB005260.Received

Leichter, J. J., and Genovese, S. J. (2006). Intermittent upwelling and subsidized growth of the scleractinian coral Madracis mirabilis on the deep fore-reef slope of Discovery Bay, Jamaica. *Mar. Ecol. Prog. Ser.* 316, 95–103. doi: 10.3354/meps316095

Leichter, J. J., Wing, S. R., Miller, S. L., and Denny, M. W. (1996). Pulsed delivery of subthermocline water to Conch Reef (Florida Keys) by internal tidal bores. *Limnol Oceanogr* 41, 1490–1501. doi: 10.4319/lo.1996.41.7.1490

Lewis, E., and Wallace, D. (1998). Program developed for CO2 system calculations. *Ornl/Cdiac-105* (United States), 1–29. doi: 10.15485/1464255

Locke, J. M., Weil, E., and Coates, K. A. (2007). A newly documented species of Madracis (Scleractinia: Pocilloporidae) from the Caribbean. *Proceedings of the Biological Society of Washington* 120, 214–226. doi: 10.2988/0006-324

Logan, A. (1988). The holocene reefs of Bermuda. *Sedimenta XI* 63.

Logan, A., and Murdoch, T. (2011). "Bermuda," in *Encyclopedia of modern coral reefs: structure, form and process, Earth Science Series*. Ed. D. Hopley (Dordrecht: Springer-Verlag), 469–486. doi: 10.1007/978-90-481-2639-2_46

Loya, Y., Eyal, G., Treibitz, T., Lesser, M. P., and Appeldoorn, R. (2016). Theme section on mesophotic coral ecosystems: advances in knowledge and future perspectives. *Coral Reefs* 35, 1–9. doi: 10.1007/s00338-016-1410-7

Y. Loya, K. A. Pulglise and T. C. L. Bridge (2019). *Mesophotic coral ecosystems* (Cham: Springer International Publishing). doi: 10.1007/978-3-319-92735-0

Manzello, D. P., Kolodziej, G., Kirkland, A., Besemer, N., and Enochs, I. C. (2021). Increasing coral calcification in Orbicella faveolata and Pseudodiploria strigosa at Flower Garden Banks, Gulf of Mexico. *Coral Reefs* 40, 1097–1111. doi: 10.1007/s00338-021-02108-8

Mass, T., Einbinder, S., Brokovich, E., Shashar, N., Vago, R., Erez, J., et al. (2007). Photoacclimation of Stylophora pistillata to light extremes: metabolism and calcification. *Mar. Ecol. Prog. Ser.* 334, 93–102. doi: 10.3354/meps334093

Mehrbach, C., Culberson, C. H., Hawley, J. E., and Pytkowicx, R. M. (1973). Measurement of the apparent dissociation constants of carbonic acid in seawater at atmospheric pressure. *Limnol Oceanogr* 18, 897–907. doi: 10.4319/lo.1973.18.6.0897

Moberg, F., and Folke, C. (1999). Ecological goods and services of coral reef ecosystems. *Ecol. Economics* 29, 215–233. doi: 10.1016/S0921-8009(99)00009-9

Muehllehner, N., Langdon, C., Venti, A., and Kadko, D. (2016). Dynamics of carbonate chemistry, production, and calcification of the Florida Reef Tract, (2009–2010): Evidence for seasonal dissolution. *AGU Publications* 30, 661–688. doi: 10.1002/2015GB005327.Received

Nash, M. C., Diaz-Pulido, G., Harvey, A. S., and Adey, W. (2019). Coralline algal calcification: A morphological and process-based understanding. *PLoS One* 14, e0221396. doi: 10.1371/journal.pone.0221396

Nash, M. C., Troitzsch, U., Opdyke, B. N., Trafford, J. M., Russell, B. D., and Kline, D. I. (2011). First discovery of dolomite and magnesite in living coralline algae and its geobiological implications. *Biogeosciences* 8, 3331–3340. doi: 10.5194/bg-8-3331-2011

Orr, J. C., Fabry, V. J., Aumont, O., Bopp, L., Doney, S. C., Feely, R. A., et al. (2005). Anthropogenic ocean acidification over the twenty-first century and its impact on calcifying organisms. *Nature* 437, 681–686. doi: 10.1038/nature04095

Page, H. N., Courtney, T. A., Collins, A., De Carlo, E. H., and Andersson, A. J. (2017). Net community metabolism and seawater carbonate chemistry scale non-intuitively with coral cover. *Front. Mar. Sci.* 4. doi: 10.3389/fmars.2017.00161

Pandolfi, J. M., Bradbury, R. H., Sala, E., Hughes, T. P., Bjorndal, K. A., Cooke, R. G., et al. (2003). Global trajectories of the long-term decline of coral reef ecosystems. *Sci. (1979)* 301, 955–958. doi: 10.1126/science.1085706

Pandolfi, J. M., Connolly, S. R., Marshall, D. J., and Cohen, A. L. (2011). Projecting coral reef futures under global warming and ocean acidification. *Sci. (1979)* 333, 418–422. doi: 10.1126/science.1204794

Perry, C. T., Murphy, G. N., Kench, P. S., Smithers, S. G., Edinger, E. N., Steneck, R. S., et al. (2013). Caribbean-wide decline in carbonate production threatens coral reef growth. *Nat. Commun.* 4, 1–7. doi: 10.1038/ncomms2409

Pinheiro, H. T., Goodbody-Gringley, G., Jessup, M. E., Shepherd, B., Chequer, A. D., and Rocha, L. A. (2016). Upper and lower mesophotic coral reef fish communities evaluated by underwater visual censuses in two Caribbean locations. *Coral Reefs* 35, 139–151. doi: 10.1007/s00338-015-1381-0

Puglise, K., Hinderstein, L., Marr, J., Dowgiallo, M., and Martinez, F. (2008). Mesophotic coral ecosystems research strategy. *Silver Spring* MD: NOAA National Centers for Coastal Ocean Science, Center for Sponsored Coastal Ocean Research, and Office of Ocean Exploration and Research, NOAA Undersea Research Program. NOAA Technical Memorandum NOS NCCOS 98 and OAR OER 2. Available at: http://purl.fdlp.gov/GPO/gpo1254.

Pyle, R. L., Copus, J. M., Pyles, R. L., and Copus, J. M. (2019). "Mesophotic coral ecosystems: introduction and overview," in *Mesophotic Coral Ecosystems, Coral Reefs of the World 12*. Eds. Y. Loya, K. A. Puglise and T. Bridge (Cham: Springer), 3–27. doi: 10.1007/978-3-319-92735-0

Sarkis, S., van Beukering, P. J. H., McKenzie, E., Brander, L., Hess, S., Bervoets, T., et al. (2013). "Total Economic Value of BERMUDA's Coral Reefs: A Summary," in *Coral reefs of the United Kingdom overseas territories*. Ed. C. R. C. Sheppard (Dordrecht: Springer Science and Business Media LLC), 201–211. doi: 10.1007/978-94-007-5965-7_15

Semmler, R. F., Hoot, W. C., and Reaka, M. L. (2017). Are mesophotic coral ecosystems distinct communities and can they serve as refugia for shallow reefs? *Coral Reefs* 36, 433–444. doi: 10.1007/s00338-016-1530-0

Slattery, M., and Lesser, M. P. (2021). Gorgonians are foundation species on sponge-dominated mesophotic coral reefs in the Caribbean. *Front. Mar. Sci.* 8. doi: 10.3389/fmars.2021.654268

Smith, S. v., and Key, G. S. (1975). Carbon dioxide and metabolism in marine environments. *Limnol Oceanogr* 20, 493–495. doi: 10.4319/lo.1975.20.3.0493

Spalding, M., Ravilious, C., and Green, E. (2002). World atlas of coral reefs. *Choice Reviews Online* 39, 39–2540. doi: 10.5860/choice.39-2540

Stefanoudis, P. V., Rivers, M., Smith, S. R., Schneider, C. W., Wagner, D., Ford, H., et al. (2019). Low connectivity between shallow, mesophotic and rariphotic zone benthos. *R Soc. Open Sci.* 6, 190958. doi: 10.1098/rsos.190958

Stefanoudis, P. V., Smith, S. R., Schneider, C., Wagner, D., Goodbody-Gringley, G., Xavier, J., et al. (2018). *Bermuda Benthic Marine Life Field Identification Guide Bermuda Benthic Marine Life Field Identification Guide Deep Reef Benthos of Bermuda: Field Identification Guide*. (Oxford, England: Nekton), 1–168. doi: 10.6084/m9.figshare.7333838.v1

Steinberg, D. K., Carlson, C. A., Bates, N. R., Johnson, R. J., Michaels, A. F., and Knap, A. H. (2001). Overview of the US JGOFS Bermuda Atlantic Time-series Study (BATS): A decade-scale look at ocean biology and biogeochemistry. *Deep Sea Res. 2 Top. Stud. Oceanogr* 48, 1405–1447. doi: 10.1016/S0967-0645(00)00148-X

Sutherland, M. G., McLean, S. J., Love, M. R., Carignan, K. S., and Eakins, B. W. (2014). *Digital Elevation Models of Bermuda: Data Sources, Processing and Analysis* (Boulder).

Suzuki, A., and Kawahata, H. (2003). Carbon budget of coral reef systems: An overview of observations in fringing reefs, barrier reefs and atolls in the Indo-Pacific regions. *Tellus B Chem. Phys. Meteorol* 55, 428–444. doi: 10.1034/j.1600-0889.2003.01442.x

Tanzil, J. T. I., Brown, B. E., Dunne, R. P., Lee, J. N., Kaandorp, J. A., and Todd, P. A. (2013). Regional decline in growth rates of massive Porites corals in Southeast Asia. *Glob Chang Biol.* 19, 3011–3023. doi: 10.1111/gcb.12279

Towle, E. K., Enochs, I. C., and Langdon, C. (2015). Threatened Caribbean coral is able to mitigate the adverse effects of ocean acidification on calcification by increasing feeding rate. *PloS One* 10, 139398. doi: 10.1371/journal.pone.0123394

Tribollet, A., Godinot, C., Atkinson, M., and Langdon, C. (2009). Effects of elevated pCO2 on dissolution of coral carbonates by microbial euendoliths. *Global Biogeochem Cycles* 23, 2006–2009. doi: 10.1029/2008GB003286

Turner, J. A., Babcock, R. C., Hovey, R., and Kendrick, G. A. (2017). Deep thinking: A systematic review of mesophotic coral ecosystems. *ICES J. Mar. Sci.* 74, 2309–2320. doi: 10.1093/icesjms/fsx085

Wilkinson, C. R. (1999). Global and local threats to coral reef functioning and existence: Review and predictions. *Mar. Freshw. Res.* 50, 867–878. doi: 10.1071/MF99121

Wilkinson, C. (2008). Status of coral reefs of the world: 2008. *Global Coral Reef Monitoring Network and Reef and Rainforest Research Centre* (Townsville, Australia).

Williams, G. J., Sandin, S. A., Zgliczynski, B. J., Fox, M. D., Gove, J. M., Rogers, J. S., et al. (2018). Biophysical drivers of coral trophic depth zonation. *Mar. Biol.* 165, 60. doi: 10.1007/s00227-018-3314-2

Wilson, R. W., Millero, F. J., Taylor, J. R., Walsh, P. J., Christensen, V., Jennings, S., et al. (2009). Contribution of fish to the marine inorganic carbon cycle. *Sci. (1979)* 323, 359–362. doi: 10.1126/science.1157972

Wolanski, E., Colin, P., Naithani, J., Deleersnijder, E., and Golbuu, Y. (2004). Large amplitude, leaky, island-generated, internal waves around Palau, Micronesia. *Estuar. Coast. Shelf Sci.* 60, 705–716. doi: 10.1016/j.ecss.2004.03.009

Wyatt, A. S. J., Leichter, J. J., Toth, L. T., Miyajima, T., Aronson, R. B., and Nagata, T. (2020). Heat accumulation on coral reefs mitigated by internal waves. *Nat. Geosci* 13, 28–34. doi: 10.1038/s41561-019-0486-4

Yeakel, K. L., Andersson, A. J., Bates, N. R., Noyes, T. J., Collins, A., and Garley, R. (2015). Shifts in coral reef biogeochemistry and resulting acidification linked to offshore productivity. *Proc. Natl. Acad. Sci. U.S.A.* 112, 14512–14517. doi: 10.1073/pnas.1507021112